Nebular metamorphosis during the post-AGB phase: multiwavelength studies

C. Sánchez Contreras[1]

[1] Department of Astrophysics, Astrobiology Center (CSIC-INTA), P.O. Box 78, E-28691 Villanueva de la Cañada, Madrid, Spain

Abstract

The processes that lead to the formation of Planetary Nebula (PN), through the short intermediate stage of pre-PN, are complex and poorly known. The biggest challenge in the study of PN formation is understanding the origin of the remarkable morphological and kinematical differences between the circumstellar envelopes (CSEs) around Asymptotic Giant Branch (AGB) stars, which result from the star mass-loss process during the AGB, and their more evolved counterparts, PPNe and PNe. While AGB CSEs expand isotropically at low velocity ($\sim$ 5–15 km/s), most PPNe and PNe have clear departures from sphericity and show fast ($>$ 100 km/s) bipolar or multipolar outflows. This spectacular metamorphosis is believed to be governed by the interaction between fast, collimated post-AGB winds (or jets), and the slow AGB CSE. In this presentation, I will review these late stages of the evolution of solar type stars and will describe some common observational techniques used to characterize the different nebular components in these objects.

1 Introduction

Intermediate mass stars ($\sim$ 1–8 $M_\odot$) evolve from the Asymptotic Giant Branch (AGB) to the Planetary Nebula (PN) phase through a short-lived ($\sim 10^3$ yr) and fascinating evolutionary stage designated as the post-AGB (post-AGB) or pre-planetary nebula (PPN) phase (Fig. 1). During the AGB phase, these stars experience an intense mass-loss process (with typical rates of $\approx 10^{-7}$–10^{-5} $M_\odot$ yr^{-1}, and even larger at the tip of the AGB) in the form of an isotropic, slow wind that leads to the formation of a thick, expanding envelope around the central star. Given the low temperatures of the AGB and early post-AGB stars ($\sim$ 2000–4000 K), the circumstellar material remains relatively cold and, therefore, is mainly composed of dust and molecules. The cessation of the large-scale mass-loss marks the end of the AGB phase and the begining of the fast, post-AGB journey during which both the star and the envelope experience important changes: the core of the AGB star, having lost its envelope, evolves

to higher temperatures and becomes progressively more compact, keeping its luminosity constant, while the envelope detaches from the star and gets more and more diluted. At the end of the post-AGB stage, the intense UV radiation field of the hot central star ionizes the circumstellar shell leading to a diffuse, emission line nebula designated as PN.
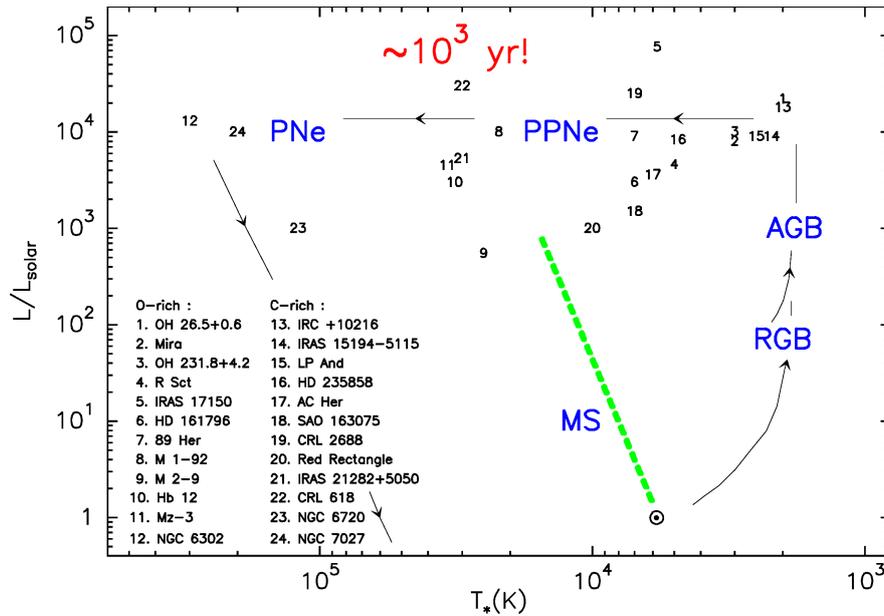

Figure 1: H-R diagram showing schematically the post-main sequence evolutionary track of a $\sim 1\,M_\odot$ star through the Red Giant Branch (RGB), the Asymptotic Giant Branch (AGB), pre-Planetary Nebula (PPN) and Planetary Nebula (PN) phases. The locus of several well studied PPNe and PNe is indicated.

At some point in the late-AGB or early post-AGB stage, a process (or processes) becomes operative that accelerates and imposes severe asymmetries upon the slow, spherical AGB winds: the spherical, slowly expanding ($V_{exp} \sim 15\,km/s$) AGB circumstellar envelope (CSE) becomes a PN with clear departures from sphericity and fast ($\geq 100\,km/s$) outflows directed along one or more axis (Fig. 2). Although there is no consensus yet for what causes this spectacular metamorphosis, fast jet-like winds have been hypothesized to play an important role (see e.g. the review paper on PNe shaping by [1]). These outflows carve out an imprint within the AGB CSE producing and shaping the fast, bipolar lobes observed in most PPNe and PNe [10].

What is the mechanism that powers and collimates post-AGB jets? When do these jets appear for the first time and what triggers their appearance? Does this depend on extrinsic factors like binarity? Do post-AGB winds have a continuous or episodic nature? How long does it take the jet launching/acceleration process? Is there a unique scenario to explain the overwhelming morphological diversity in PPNe? These are a few of the numerous fundamental issues of post-AGB evolution that remain open at present.
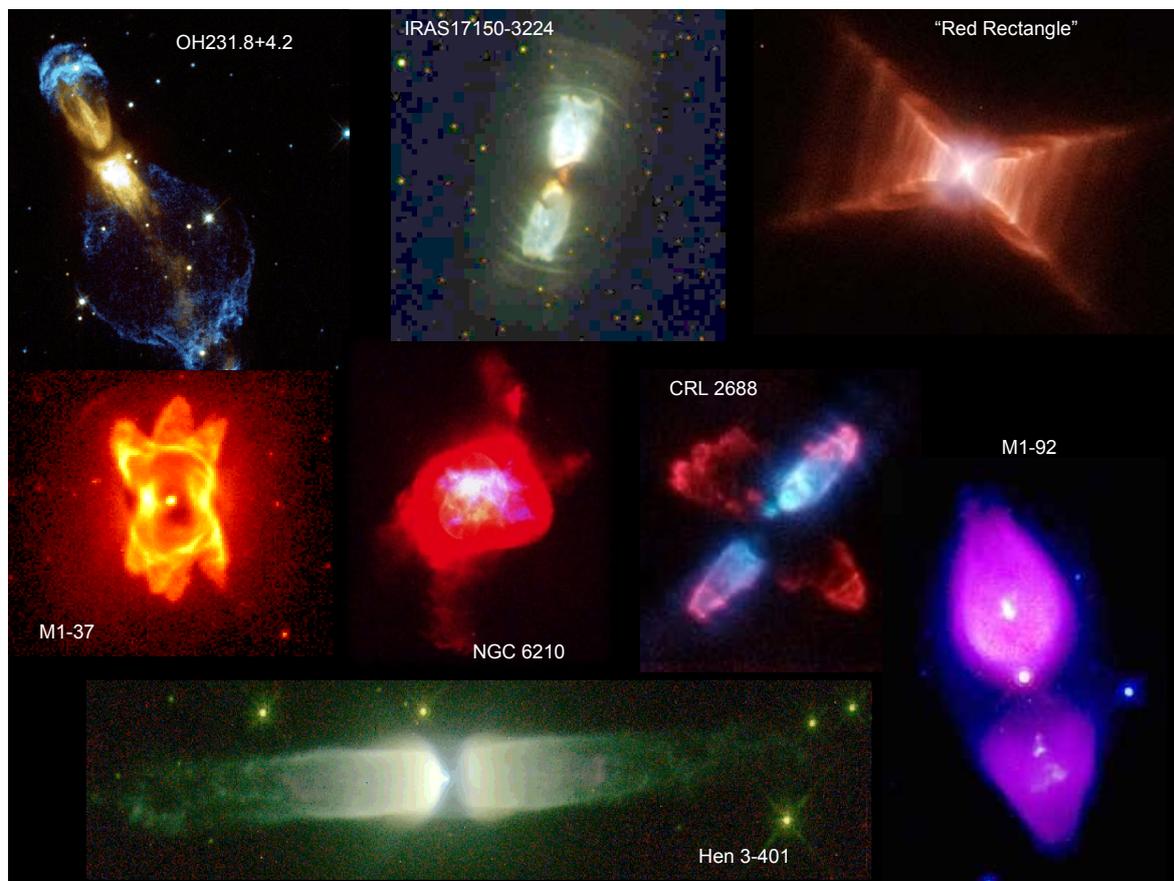
Figure 2: False color *HST* images of a selection of PPNe and young PNe.

A detailed characterization of PPNe through high-quality data for large samples is mandatory in order to answer these questions. In the following I will describe some observational techniques that are commonly used to probe different nebular components in these objects and the main results obtained.

2   Molecular envelopes: thermal CO emission observations

Rotational transitions of carbon monoxide (CO) in the millimeter wavelength (mm-wave) range are known to be the best probes of the cool, dense molecular gas of post-AGB objects, which is the major carrier of the mass, momentum and kinetic energy of their envelopes. CO mm-wave observations enable determining the density, temperature and velocity distribution (and, therefore, the dynamics) of these objects and allow us to reconstruct the mass-loss history and circumstellar evolution during the AGB and beyond.

The CO emission profiles in pPNe often display an intense narrow line core, and, in some cases, weak broader wings, indicative of slow and fast molecular outflows. Given the small

angular size of most PPNe, interferometric CO emission mapping is necessary to spatially resolve the structure of these different kinematic components. As an example, $\sim 1''$-resolution CO(J=2–1) emission maps of the well studied PPN CRL 618 are shown in Fig. 3. As for CRL 618, for the yet small number of pPNe with high angular-resolution CO maps, the line core mainly arises in the slow, roughly round remnant of the AGB CSE, whereas the wings trace fast bipolar outflows of entrained molecular gas presumably accelerated by interaction with fast post-AGB winds. These fast molecular flows are characterized by notable velocity gradients: the expansion velocity increases linearly with the radial distance to the center. Massive, equatorial tori in slow expansion are also common structures in PPNe whose origin is unclear. CRL 618 is a unique case in which it has been possible to identify an additional axial, slow component of compressed material around the optical lobes that represents the interphase between the fast, unshocked post-AGB wind and the undisturbed layers of the AGB CSE. The typical kinematical ages of the AGB haloes and fast flows are $\sim 10,000\,\mathrm{yr}$ and ≈ 100–$1000\,\mathrm{yr}$, respectively. The linear velocity gradients found in the fast post-AGB flows point to very short acceleration time scales ($\leq 100\,\mathrm{yr}$). One important result derived from CO-based studies of PPNe is that the linear momentum of the bipolar outflows is too high to be supplied by radiation pressure (e.g., [3]). This result suggests that a different mechanism for the release of linear momentum by the star other than radiation pressure, which otherwise drives AGB winds, must be at work during the post-AGB stage.

Up to date, there are very few interferometric CO mapping surveys of evolved stars. The first one is that by [9], which contained medium resolution CO maps on a sample of 47 objects. The majority of their targets ($\sim 75\%$) are AGB stars, the rest have IRAS colors typical of pPNe and PNe. The main result of this survey was that AGB CSEs have an overall spherical symmetry. A systematic study of CSEs around 46 AGB stars and 9 early post-AGB objects has been carried out recently by [5]. These authors find small-scale but remarkable asymmetries in the inner regions of some of their AGB targets. We have completed an interferometric CO emission snap-shot survey (referred to as OPACOS[1]) in a sample of 27 objects characterized in its majority by PPNe (but also including a few late-AGB stars and PNe; [14]). We report first detection of ^{12}CO (J=1–0) emission in 13 targets and confirm emission from 5 previous marginal detections, which results in almost doubling the current list of objects with published interferometric CO maps (~ 35). The molecular envelope probed by ^{12}CO (J=1–0) emission is spatially resolved for 18 (out 24) OPACOS sources; envelope asymmetries and/or velocity gradients are found in most (all?) resolved objects. Our data have been used to derive accurate target coordinates, systemic velocities and to characterize the envelope size, morphology, and kinematics. We also provide an estimate of the total molecular mass and the fraction of it contained in the fast post-AGB flows, a lower limit to the linear momentum, and the isotopic ^{12}C/^{13}C ratio. Some results from OPACOS are prensented in [15].

Although the angular resolution in still moderate in a significant fraction of objects with interferometric maps (compared to the small angular size of their envelopes), we are getting closer to establishing morphological classes and to perform statistics. For example, most PPNe have fast bipolar flows and equatorial disks expanding slowly, but a small (but

---

[1]OPACOS stands for **O**VRO **P**ost-**A**GB **CO**(1−0) emission **S**urvey.
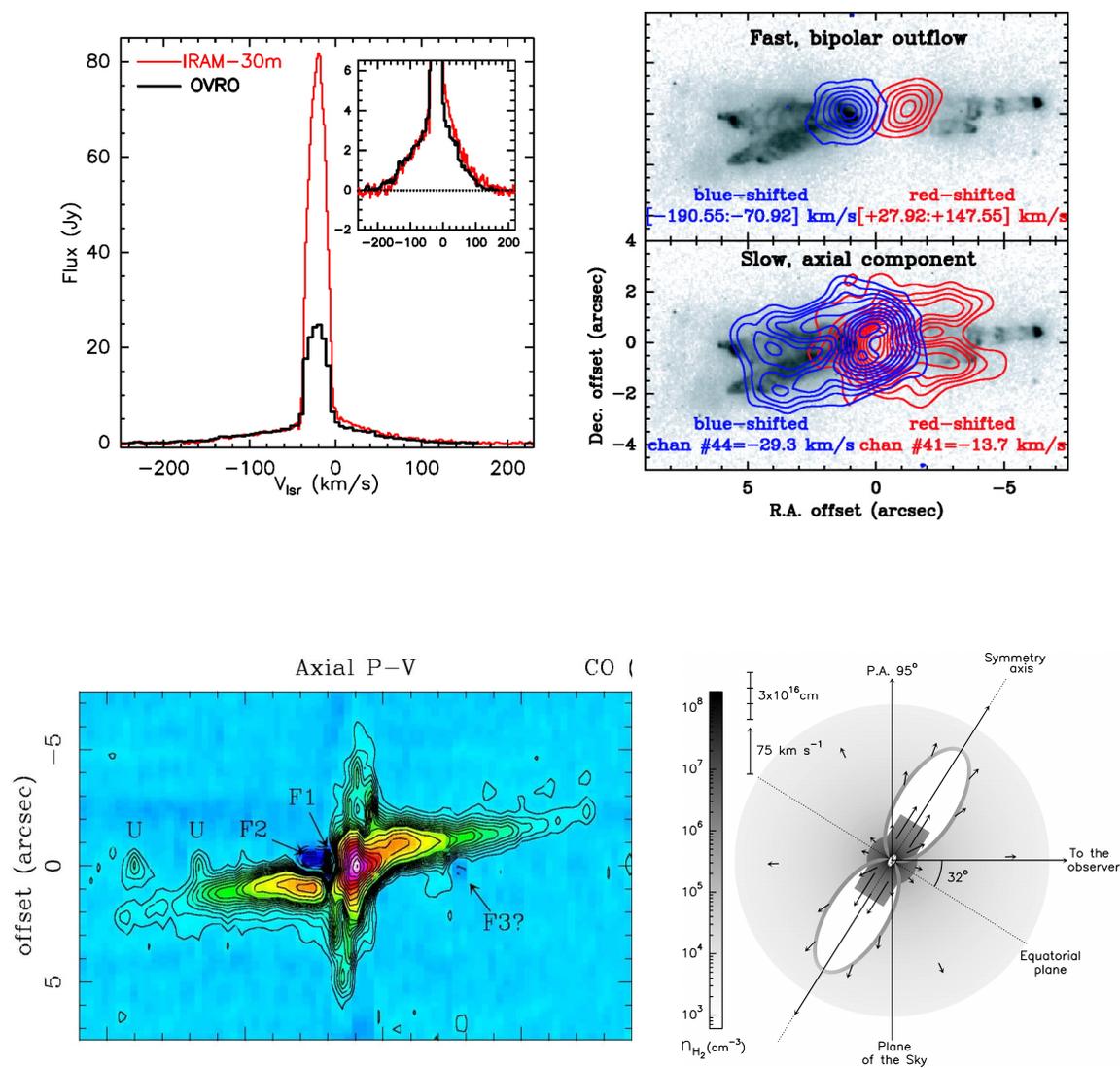
Figure 3: Figure set adapted from [18]. *Top-left*: CO J=2–1 spectral profile obtained with the OVRO millimeter interferometer (dark line) and the IRAM 30 m radio telescope (light line) of the PPN CRL 618. *Top-right*: Maps of CO J=2–1 emission integrated over selected LSR velocity intervals (indicated at the bottom of the boxes) superimposed on the *HST*/WFPC2 Hα+continuum emission image of CRL 618. Red and blue contours are used for red- and blueshifted emission with respect to the systemic velocity, respectively. *Bottom-left*: CO J=2–1 position-velocity diagrams along the nebular long axis. *Bottom-right*: Schematic drawing of the density distribution and velocity field of the molecular envelope of CRL 618 derived from modeling of the CO data.

increasing) number also show multi-directed and nearly orthogonal fast bipolar flows (as those observed in the PPN CRL 2688 [6], and the one discovered in our OPACOS target IRAS 19255+2123 [14]); so far, only one confirmed keplerian rotation disk, predicted by some wind collimation theories, has been found in the PPN "The Red Rectangle" [4].

3 Dust and $\sim$10,000 K gas component: optical imaging and spectroscopy

Observations of PPNe/PNe in the optical wavelength range are used to study the dust distribution in their refection nebulae and the dark equatorial waists, and the mid-excitation ($\sim$ 10,000 K) gas component. The latter partially results from the increasing UV stellar radiation field that penetrates the envelope (leading to the emergence and progressive growing of a nuclear HII region around the star) and the heating produced by shocks developed in the hydrodynamic 'post-AGB+AGB' wind interaction.

3.1 Imaging

One of the main problems trying to unveil the post-AGB shaping agents is the puzzling morphological diversity found: almost every object appears to be unique (Fig. 1). Large, unbiased samples of PPNe/PNe are needed for morphological classification and to obtain robust statistical results. Progress also requires high-angular resolution because most PPNe are small ($< 5''$–$10''$) with rich structure at a scale $\leq 0.1''$ (jets, knots, disks, arcs..) and because the shaping mechanism operates close to the central star, $< 10^{16}$ cm (see e.g., [1]).

Using the *HST*, we have carried out an optical/near-infrared imaging survey of generally young PPNe, using a large (~ 300), morphologically unbiased sample mostly constructed from catalogs of OH/IR stars (evolved, visually faint, mass-losing stars with dense CSEs, showing generally double-peaked OH maser emission). The IRAS spectral energy distributions (SEDs) of a large fraction of these objects indicate a lack of hot dust (25-to-12 μm flux ratio F25/F1 > 1, implying a lack of dust hotter than ~ 450 K) and therefore cessation of the dense AGB mass-loss process less than a few hundred years ago. Our main goal is probing, in their infancy, the physical processes that produce asphericity. Our discoveries of objects having well-resolved geometric structures and our new morphological classification system are presented in [11] – see also Fig. 4. The wide variety of aspherical morphologies which we have found for PPNe are qualitatively similar to those found for young PNe in previous surveys. We also find prominent halos surrounding the central aspherical shapes in many of our objects; these are direct signatures of the undisturbed circumstellar envelopes of the progenitor AGB stars. Although the majority of these have surface brightness distributions consistent with a constant mass-loss rate with a constant expansion velocity, there are also examples of objects with varying mass-loss rates. As in our surveys of young PNe, we find no round PPNe. The similarities in morphologies between our survey objects and young PNe supports the view that the former are the progenitors of aspherical PNe. This suggests that the primary shaping of a PN does not occur during the PN phase via the fast radiative wind
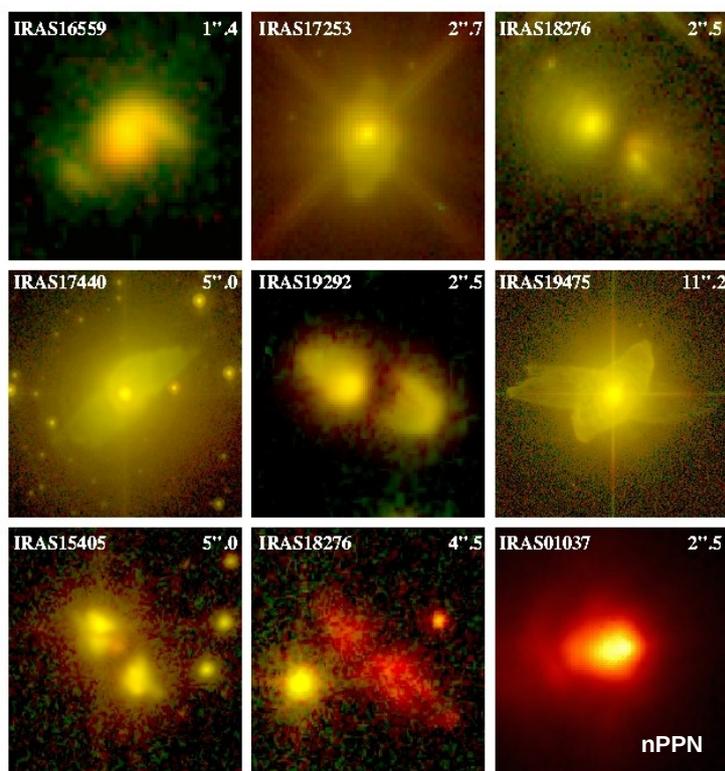
Figure 4:   False color images of several objects from our *HST* imaging survey of PPN candidates [11]. Our new morphological classification establishes four main classes of nebular shapes: bipolar (B), multipolar (M), elongated (E), and irregular (I), as well as a number of secondary structural features, for example, the presence of a dark obscuring waist across the center of the nebula, direct visibility of the central star in the optical or NIR, open or close lobe ends, etc.

of the hot central star, but significantly earlier in its evolution.

We have also carried out an *HST* imaging program to study 48 objects which, from the evolutionary standpoint, bracket the PPN phase. The aspherical structure in the images of spatially resolved nascent PPN, $\sim 30\%$ of the sample, is generally one-sided when collimated structures are seen (Fig. 4, bottom-right panel). This is very different from that observed in normal PPNe, which show diametrically-opposed, limb-brightened lobes. Finally, from a recent morphological study based on *HST* images of young PNe and PNe (by [12]) one additional morphology class has been found: a small fraction of the objects observed (4/117) display spiral-arm structure. Kinematical studies now remain to be done in these objects for dealing with projection effects, and recovering full 3D geometry of these enigmatic new objects.

3.2 Spectroscopy

Our current (very limited) knowledge of post-AGB evolution and, more particularly, of post-AGB winds is derived mainly in two ways. The first is *indirect* – based on the effects of the post-AGB winds on the CEs formed in the previous AGB phase. Most PPNe/PNe show extended lobes with, often, bow-shaped features at their tips that are visible through optical recombination and forbidden emission lines. Spectroscopic observations have been crucial for understanding the origin of these regions and building up the current picture of post-AGB evolution. From long-slit spectra we derive a) the kinematics of these regions, which are rapidly expanding with, usually, the velocity (V) linearly increasing with the distance to the central star (r); this linear dependence of V with r allow us to recover the 3D nebular structure (Fig. 5); b) the excitation mechanism and physical conditions (electron density and temperature) of these regions from the analysis of diagnostic line ratios and their spatial variation across the nebula. Such studies indicate that these regions are excited by the passage of fast ($\geq 100\,\mathrm{km\ s}^{-1}$) shocks. (See e.g. [16, 17, 20] and [21], for some examples of studies based on optical spectroscopy). From these results we *infer* the existence of fast, post-AGB winds that interact hydrodynamically with the AGB CE leading to the formation of shocks and, ultimately, to the acceleration and shaping of the nebular material.

Direct detection of post-AGB winds is limited to a very few objects. In some cases (e.g. He 3-1475, Fig. 6), there is Balmer and forbidden line emission arising in a set of compact, shock-excited regions located along the nebular axis. These "knots", which usually move away from the star at high velocity, are thought to result from the propagation of backward shocks in the post-AGB wind itself, *suggesting* that post-AGB winds are collimated and directed along the nebular axis. In some PPNe/PNe, fast, post-AGB winds are also revealed by P-Cygni profiles close to the central star (e.g., [19]). Recently, the spatio-kinematic structure of pristine post-AGB winds has been directly studied for the first time in the PPN He 3-1475, through the analysis of P-Cygni absorption features in STIS long-slit Hα spectra (Fig. 6 and [13]). For the central slit, we observe two distinct absorption features which we interpret as resulting from neutral or partially-ionized fast- and ultra-fast outflows within the nebular lobes absorbing the Hα and stellar photons scattered by the dust in the lobe walls. The ultra-fast ($2300\,\mathrm{km\ s}^{-1}$) wind is highly collimated as deduced from the *absence of feature 2 in the outer slits*, and shows a large velocity gradient (the outermost parts are the fastest). These properties are best explained by magneto-hydrodynamical wind collimation models [8] and rule out, e.g., collimation via conical shocks [2].

Our study on He 3-1475 demonstrates the effectiveness of optical spectroscopy in probing the elusive post-AGB winds and understanding their collimation mechanism. According to this, we are carrying out long-slit spectroscopic observations with *HST*/STIS of a sample of PPNe with intense, ongoing post-AGB jet activity (GO 11634, PI: Sánchez Contreras). Our aim is to identify and directly study post-AGB winds with high-spatial resolution near the launching site, which is needed to discriminate between different wind collimation theories and to understand the nebular evolution beyond the AGB. A secondary goal is to study the spatio-kinematic structure of the extended, shocked lobes and their connection with the small-scale structures near the star.
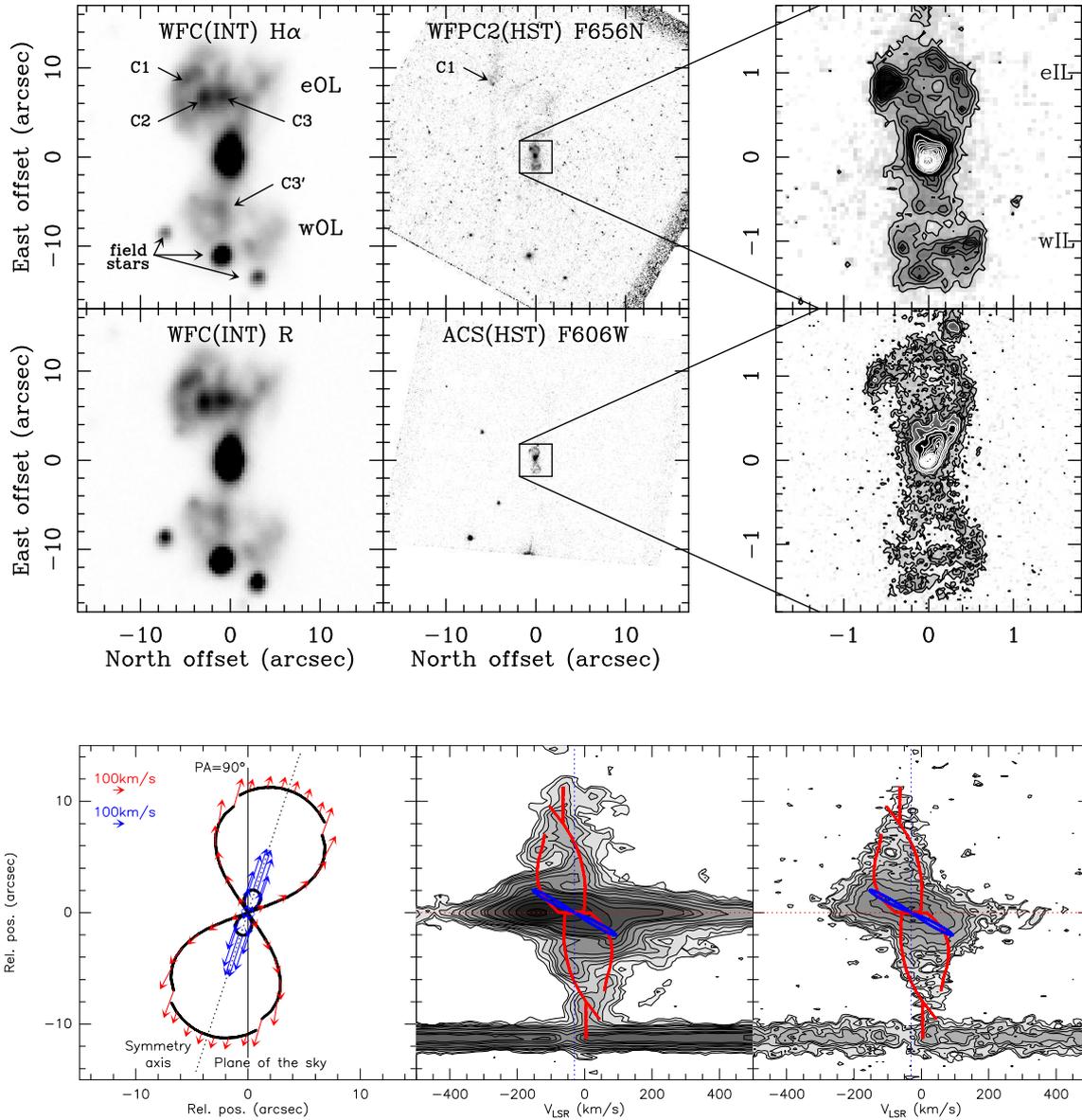
Figure 5: Figure adapted from [20] – see also [21]. *Top*: (*Left*) Ground-based images of the PPN M 2-56 through the narrow Hα and *R* broad-band filters; (*Middle*) Images obtained with the *HST* through the F656N (Hα) and F606W filters; (*Right*) Inset of the *HST* images showing the small-scale structure of the inner nebular lobes. *Bottom*: (*Left*) Schematic geometry of M 2-56 deduced from the fit of a spatio-kinematic model to the Hα long-slit spectra along the nebula symmetry axis. This plot represents a cut of the nebula by a plane perpendicular to the plane of the sky in the direction of PA90. The velocity field in is indicated by arrows. (*Middle and Right*) Hα spectrum along PA = 90º as observed in 1998 and 2000. The position-velocity diagrams resulting from the model fitting are superimposed.
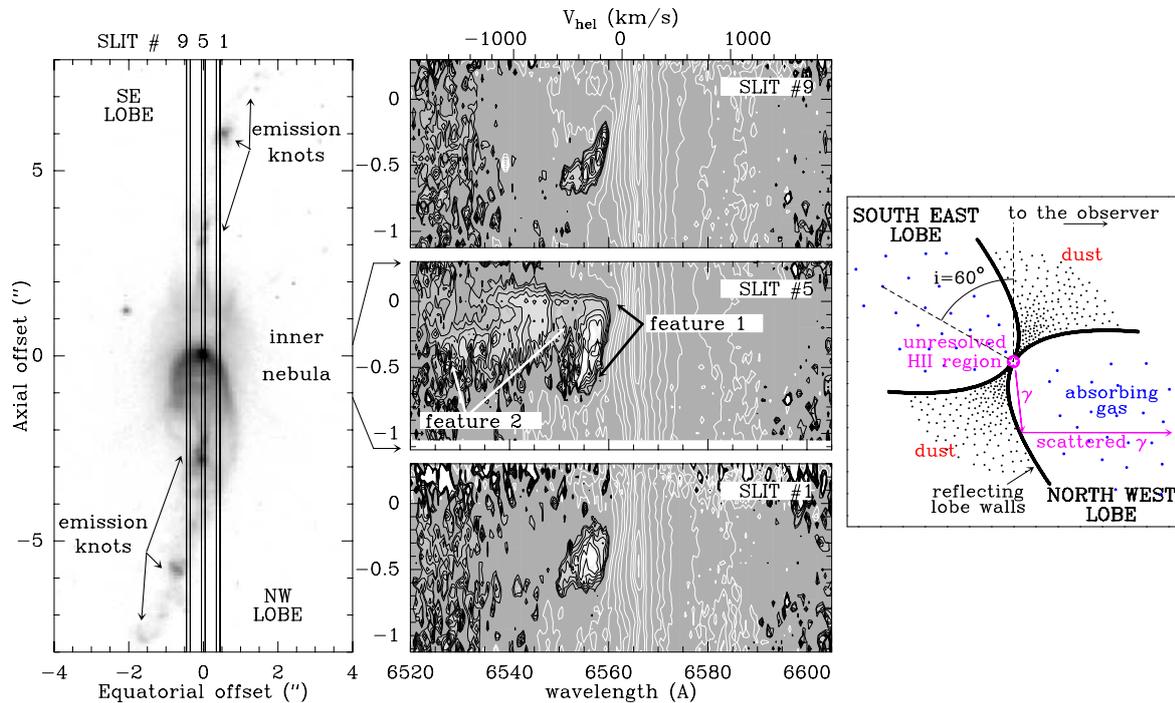
Figure 6: Figure set adapted from [13]. *Left*: WFPC2, Hα+continuum image of He 3-1475; three of the nine 0.1″-wide slits used for the STIS observations are superimposed. *Center*: STIS Hα P Cygni spectra (divided by the continuum) for each slit in the 1″-*inner* nebula. In the central slit (#5), two blue-shifted absorption features are observed (black contours); feature 2 is not present in the outer slits. *Right*: Sketch of our interpretation of the STIS data: the H$_\alpha$ emission from the compact HII region and the stellar continuum are scattered by dust in the lobe walls; the absorption features are produced by gas inside the reflecting lobes.

Finally, I would also like to strees the importance of multi-epoch imaging and spectroscopic observations of PPNe, not only to measure the expansive proper motions of the fast lobes and their shock fronts, which is crucial to understand the wind interaction process, but also to identify short-duration mass-loss events or rapid changes in the nuclear regions related to current post-AGB jet activity (see e.g. [20, 21]).

4 Final remarks

Although there are still many open questions concerning post-AGB evolution, we are making significant progress in characterizing the different components of PPNe, their origin, and their mutual connections. At this respect, multi-wavelength studies are of utmost importance since they provide us with a global view of the complex processes mediating the AGB-to-PN transition. In the next years, our observational capabilities will improve considerably with

the advent of new facilities like, e.g., ALMA and JWST, which are particularly well suited to study the intricate phenomenology of these objects and, therefore, hold the promise to unprecedented advances in this field. As the number of late-AGB, PPNe, and yPNe with high-quality data increases, we will overcome the current lack of large, unbiased samples (including different nebular & stellar evolutionary stages, chemistry types, initial masses, etc) with high-quality data needed to search for correlations between the different nebular and stellar parameters derived from multi-wavelength data and to obtain robust statistical results. Finally, the joint efforts between observers and theoreticians are also increasing and starting to give their first fruits, for example, pointing to magneto-centrifugal jet launching/collimation mechanisms and favoring short-lived (bullet-type), episodic fast ejections rather than continous post-AGB winds [7] and references therein.

Acknowledgments

References

[1] Balick, B., & Frank, A. 2002, ARA&A, 40, 439

[2] Borkowski, Blondin, & Harrington 1997, ApJ 482, L97

[3] Bujarrabal, V., Castro-Carrizo, A., Alcolea, J., & Sánchez Contreras, C. 2001, A&A, 377, 868

[4] Bujarrabal, V., Neri, R., Alcolea, J., & Kahane, C. 2003, A&A, 409, 573

[5] Castro-Carrizo, A., et al. 2007, Why Galaxies Care About AGB Stars: Their Importance as Actors and Probes, 378, 199

[6] Cox, P., Lucas, R., Huggins, P. J., Forveille, T., Bachiller, R., Guilloteau, S., Maillard, J. P., & Omont, A. 2000, A&A, 353, L25

[7] Dennis, T. J., Cunningham, A. J., Frank, A., Balick, B., Blackman, E. G., & Mitran, S. 2008, ApJ, 679, 1327

[8] García-Segura G., 1997, ApJ 489, L189

[9] Neri, R., Kahane, C., Lucas, R., Bujarrabal, V., & Loup, C. 1998, A&ASS, 130, 1

[10] Sahai, R., & Trauger, J. T. 1998, AJ, 116, 1357

[11] Sahai, R., Morris, M., Sánchez Contreras, C., & Claussen, M. 2007, AJ, 134, 2200

[12] Sahai, R., Morris, M., & Villar, 2010, AJ, submitted

[13] Sánchez Contreras, C., & Sahai, R. 2001, ApJ, 553, L173

[14] Sánchez Contreras, C., & Sahai, R. 2010, A&A, submitted

[15] Sánchez Contreras, C., & Sahai, R. 2011, these proceedings

[16] Sánchez Contreras, C., Bujarrabal, V., Miranda, L. F., & Fernández-Figueroa, M. J. 2000, A&A, 355, 1103

[17] Sánchez Contreras, C., Sahai, R., & Gil de Paz, A. 2002, ApJ, 578, 269

[18] Sánchez Contreras, C., Bujarrabal, V., Castro-Carrizo, A., Alcolea, J., & Sargent, A. 2004, ApJ, 617, 1142

[19] Sánchez Contreras, C., Sahai, R., Gil de Paz, A., & Goodrich, R. 2008, ApJS, 179, 166

[20] Sánchez Contreras, C., Cortijo-Ferrero, C., Miranda, L. F., Castro-Carrizo, A., & Bujarrabal, V. 2010, ApJ, 715, 143

[21] Sánchez Contreras, C., Cortijo-Ferrero, C., Miranda, L. F., Castro-Carrizo, A., & Bujarrabal, V. 2011, these proceedings